Cigarette smoke-induced extracellular vesicles from dendritic cells alter T-cell activation and HIV replication

Ashley E. Russell [a,b,*,1], Zhaohao Liao [a,1], Mercedes Tkach [c], Patrick M. Tarwater [d], Matias Ostrowski [e], Clotilde Théry [c], Kenneth W. Witwer [a,f,g,*]

[a] Department of Molecular and Comparative Pathobiology, The Johns Hopkins University School of Medicine, Baltimore, MD, United States
[b] Department of Biology, School of Science, Penn State Erie, The Behrend College, Erie, PA, United States
[c] INSERM U932, Institut Curie Centre de Recherche, PSL Research University, Paris, France
[d] Department of Epidemiology, The Johns Hopkins University Bloomberg School of Public Health, Baltimore, MD, United States
[e] Instituto INBIRS, Universidad de Buenos Aires-CONICET, Buenos Aires, Argentina
[f] Department of Neurology, The Johns Hopkins University School of Medicine, Baltimore, MD, United States
[g] The Richman Family Precision Medicine Center of Excellence in Alzheimer's Disease, The Johns Hopkins University School of Medicine, Baltimore, MD, United States

ARTICLE INFO

ABSTRACT

Despite decreased rates of tobacco smoking in many areas, cigarette smoking remains a major contributor to many health problems. Cigarette smoking can reduce immune system functioning while concurrently increasing inflammation. Dendritic cells in the lung exposed to cigarette smoke become stimulated and go on to activate T-cells. Extracellular vesicles (EVs) are nano-sized particles released by cells. They participate in intercellular communication by transferring functional proteins and nucleic acids to recipient cells and have been implicated in immune responses. For example, they can display MHC-peptide complexes to activate T-cells. In the current study, we sought to understand the role of cigarette smoke extract (CSE) on dendritic cell-derived EVs and their capacity to activate and differentiate T-cells. Primary human dendritic cells (iDCs) were exposed to CSE and EVs were separated and characterized. We exposed autologous primary CD4 + T-cells to iDC-EVs and observed T helper cell populations skewing towards Th1 and Th17 phenotypes. As HIV + individuals are disproportionately likely to be current smokers, we also examined the effects of iDC-EVs on acutely infected T-cells as well as on a cell model of HIV latency (ACH-2). We found that in most cases, iDC-CSE EVs tended to reduce p24 release from the acutely infected primary T-cells, albeit with great variability. We did not observe large effects of iDC-EVs or direct CSE exposure on p24 release from the ACH-2 cell line. Together, these data suggest that iDC-CSE EVs have the capacity to modulate the immune responses, in part by pushing T-cells towards Th1 and Th17 phenotypes.

1. Introduction

Although rates of cigarette smoking have declined in many regions, cigarette smoking is still a major detriment to global public health (Creamer et al., 2019). Smoking introduces a variety of carcinogenic and pre-carcinogenic substances into the user, and aside from well-known deleterious effects on the lungs and cardiovascular system, cigarette smoking also alters immune system function by changing the reactivity and differentiation of T-cells (Talhout et al., 2011; Lee et al., 2012; Onor et al., 2017; Strzelak et al., 2018). Isolated immune cells from lungs of smokers show impaired immunoproteasome activity and reduced

expression of major histocompatibility complex (MHC) proteins (Kammerl et al., 2016). Cigarette smoking can have both pro-inflammatory and immunosuppressive effects and has previously been shown to alter T-cell activation (Tollerud et al., 1989; Sopori and Kozak, 1998; Qiu et al., 2017). Many studies report alterations of T helper (Th) cell (Th1, Th2, and Th17) populations in smokers when compared with non-smokers, although some of these findings are conflicting. Some reports conclude that cigarette smoking increases Th1/Th17 profiles and suppresses Th2 (Harrison, 2008; Vargas-Rojas et al., 2011), while others observe that smoking increases Th2 and suppresses Th1/Th17 differentiation (Cozen et al., 2004; Van Hove et al., 2008; Torres de Heens

---

et al., 2009). Factors including the methodologies and techniques employed for *in vitro* cigarette smoke extract (CSE) preparation, as well as underlying health conditions present in *in vivo* studies, may contribute to these discrepancies.

Dendritic cells (DCs) are professional antigen presenting cells that can modulate T-cell responses. Pulmonary DCs residing in the mucosal lining of the respiratory tract are exposed to inhaled substances. These DCs can become activated and migrate to the nearest lymph node, where they activate T-cells. Inhaled cigarette smoke has been shown to alter DC maturation and activation capacity, as well as the ability of exposed DCs to activate T cells (Vassallo et al., 2005; Robbins et al., 2008; Feigin et al., 2014; Le Rouzic et al., 2016).

Cigarette smoking has also been shown to impair the immune system's ability to respond to pathogens, including viruses. As for other drugs of abuse, rates of cigarette smoking are 2- to 4-fold higher in HIV + populations (Reynolds, 2009; Vijayaraghavan et al., 2014). Cigarette smoke (CS) increases expression of the primary HIV receptor CD4 (Chinnapaiyan et al., 2018) as well as CCR5 (Wang and He, 2012), an HIV co-receptor (Bleul et al., 1997). Both HIV Tat protein and CS suppress cystic fibrosis transmembrane conductance regulator function, which impacts mucociliary clearance from the lung, in turn increasing the susceptibility of these patients to lung infections (Chinnapaiyan and Unwalla, 2015; Chinnapaiyan et al., 2018). When compared with HIV-smokers, HIV + individuals with a history of smoking show greater susceptibility to lung damage and deficiencies in gas exchange (Diaz et al., 1999). Further, CS exposure has been shown to induce oxidative stress and increase HIV replication (Rao et al., 2016). CS may thus contribute to susceptibility to HIV infection, spread, and pathogenesis. Additionally, HIV-infected DCs provoke secretion of immunosuppressive cytokines from T-cells and further impair immune system functionality (Manches et al., 2014).

Also involved in immune responses are extracellular vesicles (EVs). EVs are small, lipid bilayer-delimited biological nanoparticles (usually tens to hundreds of nanometers in diameter) that are released by all cells. EVs have various physiological functions, such as cellular removal of toxic or excess molecules and trophic support, but they have received increasing attention because of perceived roles in intercellular signaling. Specifically, molecular constituents of EVs may stimulate signaling pathways by interacting with or delivering cargo into recipient cells. Here, we sought to characterize the effects of CSE on primary iDC activation, extracellular vesicle (EV) release, and EV-mediated activation of autologous primary T-cells. We also assessed the effects of iDC-derived EVs (iDC-EVs) on both acutely infected primary T-cells and an HIV latency model.

2. Materials and methods

2.1. Isolation of PBMCs from healthy donor Leukopaks

Human CD14+ and CD4+ peripheral blood mononuclear cells (PMBCs) were isolated from Leukopaks of healthy donors obtained from the New York Blood Center using SepMate PBMC Isolation Tubes (STEMCELL Technologies; Catalog #85450) as per the manufacturer's protocol. Briefly, 15 mL Ficoll-Paque Plus (GE Healthcare, Catalog # 17-1440-13) was added to each SepMate tube and centrifuged at 1200 x g for 1 min. Leukocyte-enriched blood was diluted to 350 mL with dilution buffer (1x phosphate buffered saline (PBS), 2% fetal bovine serum (FBS), 2 mM Ethylenediaminetetraacetic acid (EDTA)), and 35 mL was gently added to each SepMate tube, then centrifuged at 1200 x g for 10 min. PBMC-containing supernatant was then transferred to a new 50 mL Falcon tube, diluted with dilution buffer to 50 mL, and centrifuged at 400 x g for 10 min. After decanting the supernatant, red blood cell lysis buffer (4.15 g NH_4CL, 0.5 g $KHCO_3$, 0.15 g EDTA in 450 mL H_2O; pH adjusted to 7.2–7.3; volume adjusted to 500 mL and filter-sterilized (Liao et al., 2017) was added to the cell pellets, and incubated at 37 °C for 5 min. Cells were pelleted at 1500 x g for 5 min and washed once

more with dilution buffer.

2.2. Isolation of CD14+ and CD4+ cells

Total isolated PBMCs were counted using the Muse Cell Counter (Millipore) and resuspended in dilution buffer to a concentration of 125 × 10^6 cells/mL. Human CD14 MicroBeads (Miltenyi Biotec, Catalog # 130-050-201) were added to the cells at a concentration of 5 μL/10^7 cells, and incubated at 4 °C for 20 min. Cells were then diluted with dilution buffer and centrifuged at 1500 x g for 5 min. Cell pellets were resuspended in 4 mL dilution buffer and loaded onto LS Columns (Miltenyi Biotec, Catalog # 130-042-401) placed into a MACS® Magnetic Separator (Miltenyi Biotec). The LS column was washed three times with dilution buffer. Cells retained in the column (CD14+ cells) were released and washed once with dilution buffer. Cells in the flow-through fraction were pelleted and resuspended in dilution buffer at a concentration of 250 × 10^6/mL. Human CD4 + T Cell Biotin-Antibody Cocktail (Miltenyi Biotec, Catalog # 130-096-533) was added at a concentration of 5 μL/10^6 cells and incubated at 4 °C for 10 min. Next, human CD4 + T Cell MicroBead Cocktail (Miltenyi Biotec, Catalog # 130-096-533) was added to the cells at a concentration of 10 μL/10^6 cells and incubated at 4 °C for 15 min. The total volume of cells was then brought up to 4 mL with dilution buffer, and cells were passed through a new LS column in the MACS Magnetic Separator. The column was then washed three times with dilution buffer, with the CD4+ cells in the flow-through fraction. Cells were washed and suspended in freezing medium (90 % FBS, 10 % DMSO) at a concentration of 10^7 cells/mL. Cells were stored at −80 °C overnight and transferred to a liquid nitrogen tank the next day.

2.3. Immature dendritic cell differentiation

Due to the high variability of CD14+ cell yield with each Leukopak, varying cell numbers and volumes were utilized. When plating densities were below 30 × 10^6, cells were cultured in T25 flasks with 10 mL; isolations with higher plating densities were cultured in T75 s or T125 s with 20−30 mL media. CD14+ cells were cultured in RPMI 1640 medium with 10 % FBS or human AB serum, containing 100 ng/mL GMCSF and 50 ng/mL Human IL-4 at concentration of approximately 10^6 cells/mL. Culture medium was changed every two days, and cells were differentiated for 5–6 days before further treatment. Cell morphology was monitored daily. At days 5–6, cells usually have characteristic immature dendritic cell (iDC) morphology: irregular cell shape, cell dendrite formation, cell colony formation, and a mixture of attached and suspension cells.

2.4. Preparation of cigarette smoke extract (CSE) media

Cigarette smoke extract (CSE) was made by using a lab-designed and assembled apparatus as previously described (Bernstein et al., 2019). Briefly, 25 mL of serum-free AIM-V (Gibco, Catalog # 12055-091) was aliquoted into a 50 mL conical tube and sealed with parafilm. Next, a 5 mL serological pipette (cut at the 3.5 mL marking) was inserted through the parafilm, down into the culture medium, and sealed in place with parafilm. This apparatus was connected to one end of an approximately 0.75 m length of Tygon tubing (Cole-Parmer, Catalog # 06509-17), which was fed through a Cole-Parmer Masterflex L/S peristaltic pump. A 1 mL pipette tip was inserted into the other end of the Tygon tubing. One Spectrum research-grade cigarette (filter intact) was lit and inserted into the wide end of the 1 mL pipette tip. The cigarette was then continuously smoked by the peristaltic pump (speed setting 32) into the cell culture medium. The product was considered to be 100 % CSE medium.

2.5. Immature dendritic cell CSE exposure and EV concentration

By day 6, CD14+ cells displayed characteristic iDC morphology and

were ready for CSE (or control) exposures. iDCs were treated every 24 h via a complete media change, with fresh serum-free AIM-V medium or 50 % CSE AIM-V medium for 5 days. Conditioned media collected each day from control and CSE-exposed iDCs were centrifuged at 1,000 x *g* for 5 min. Any cells in suspension were pelleted and resuspended in fresh medium (control or 50 % CSE) and returned to their respective flasks for continued culturing for 5 total days of control or 50 % CSE exposure. Conditioned media were then stored at 4 °C for the duration of the experiment, then pooled and subjected to differential centrifugation in a Sorvall WX 80+ ultracentrifuge using the AH-629 swinging bucket rotor (k-factor: 284.0): 2000 x *g* for 20 min, 10,000 x *g* for 40 min, and 100,000 x *g* for 90 min. After each centrifugation, the UC pellet was resuspended in approximately 1 mL PBS, designated as 2k, 10k, and 100k pellet, respectively, and stored at −80 °C until use.

2.6. Western blot analysis

Samples were lysed with RIPA buffer (Cell Signaling Technology, Catalog # 9806S) with 1x cOmplete™ Protease Inhibitor Cocktail (Sigma, Catalog #11697498001) (10 u L for EV-enriched pellets, and 5 mL for pellets of approximately 30×10^6 cells) on ice for 30 min. Cell pellet lysates were briefly centrifuged at 12,000 rpm for 5 min to remove debris. Protein concentrations from cell lysates were determined by BCA (Thermo Fisher Scientific, Catalog # 23225), and 10 µg protein was loaded per lane. In addition, 20 µL of the lysed 2k, 10k, and 100k ultracentrifugation pellets were loaded per lane. Samples containing 1x Laemmli Gel Loading Buffer (BioRad Catalog # 1610747) were placed into a heating block at 95 °C for 5 min, then placed on ice for 3 min. Samples were loaded onto a 10 % Tris-Glycine SDS polyacrylamide gel (BioRad Catalog # 5678034) and subjected to electrophoresis at 100 V for 1 h 40 min in 1x Tris/Glycine/SDS running buffer (BioRad Catalog # 161-0732), followed by transfer to Immun-Blot PVDF Membrane (Bio-Rad, Catalog # 1620177) in 1x Tris/Glycine transfer buffer at 30 V for 1 h at 4 °C. The membrane was then blocked for 1 h with 5% Blotting-Grade Blocker (BioRad, Catalog # 1706404) in PBST (1x PBS with 0.05 % Tween-20). Blots were probed overnight at 4 °C with primary antibodies to CD63 (BD Pharmingen, Catalog # 556019, Clone H5C6), CD81 (Santa Cruz, Catalog # sc-166029), Syntenin-1 (Santa Cruz, Catalog # sc-515538) GM130 (Abcam, Catalog # ab31561, polyclonal), and Calnexin (Abcam, Catalog # ab22595, polyclonal). The next day, membranes were washed four times with PBST for 5 min each, then incubated with HRP-conjugated secondary antibodies (m-IgGk BP-HRP, Santa Cruz, Catalog # sc-516102; mouse anti-rabbit IgG-HRP, Santa Cruz, Catalog # sc-2357) for 1 h at room temperature. After four five-minute washes with PBST, blots were developed by incubation in SuperSignal West Pico Chemiluminescent Substrate for 5 min on an orbital shaker (Thermo Fisher Scientific, Catalog # 34580), and exposed with Amersham Hyperfilm (GE Healthcare Biosciences Corp, Catalog # 28906838).

2.7. Electron microscopy

Samples were adsorbed (10 u L) to glow discharged (EMS GloQube) carbon coated 400 mesh copper grids (EMS), by floatation for 2 min. Grids were quickly blotted then rinsed in 3 drops (1 min each) of TBS. Grids were negatively stained in 2 consecutive drops of 1% uranyl acetate with tylose (1% UAT, double filtered, 0.22 um filter), blotted, then quickly aspirated to get a thin layer of stain covering the sample. Grids were imaged on a Phillips CM-120 TEM operating at 80 kV with an AMT XR80 CCD (8 megapixel).

2.8. Particle concentration measurement

A NanoSight NS500 instrument with 405 nm laser (Malvern Instruments, Amesbury, UK) was calibrated with standard beads according to the manufacturer's instructions prior to particle measurement.

Appropriate dilutions of samples were made by using purified distilled water. At least five 20-second videos were recorded for each sample with a camera setting of 11 or 12. Data were analyzed at a detection threshold of 5 using NanoSight software version 3.1.

2.9. EV immune phenotyping by flow cytometry

The MACSPlex Exosome Kit was used (Miltenyi Biotec, Catalog # 130-108-813) as per the manufacturer's instructions, following the overnight protocol for 1.5 mL reagent tubes. Briefly, 0.5–2.6×10^{10} total particles suspended in 120 µL PBS were incubated with 15 µL Capture Beads and incubated overnight on an orbital shaker, protected from light. The following day, 500 µL MACSPlex Buffer was added to each tube and centrifuged at 3000 x g for 5 min. 500 µL supernatant was removed from each tube, 15 µL MACSPlex Detection Reagent (mixture of fluorophore-labeled antibodies directed against CD63, CD9, and CD81) was added, and tubes were incubated for 1 h at room temperature on an orbital shaker. 500 µL MACSPlex Buffer was again added to each tube, centrifuged at 3000 x g for 5 min, and 500 µL supernatant was removed. 500 µL of fresh MACSPlex buffer was added to each tube and incubated at room temperature for 15 min. Tubes were again centrifuged at 3000 x g for 5 min, and 500 µL supernatant was removed. Lastly, 100 µL MACSPlex Buffer was added to each tube, and flow cytometry was performed with a BD Fortessa Flow Cytometer. The following settings were used: FSC-Log 220; SSC-Log 200; FITC-Log 467; PE-Log 390; APC-Log 566. FlowJo Software (FlowJo, LLC) was used to analyze the data. Media and isotype controls were subtracted from the acquired event data and markers with negative expression values were excluded from the analysis. Total fluorescence for all positive markers from each set of iDC-EVs (control and CSE) was summed, and percent fluorescence for individual markers was calculated.

2.10. Flow cytometry of immune cells

Previously isolated CD4 + T cells were thawed from liquid nitrogen and cultured overnight in 10 % FBS, RPMI-1640 cell culture medium. Cells were harvested, washed once with serum-free medium, and aliquoted into a 96-well plate (4×10^5 cells/well). Equal volumes or numbers of vesicles were added to correspondent wells and mixed thoroughly. After two days in culture, GolgiPlug (1 µL/mL) (BD Biosciences, Catalog # 555028) and GolgiStop (0.7 µL/mL) (BD Biosciences, Catalog # 554724) were added to the cells and mixed thoroughly. Cells were cultured for 4 additional hours before being harvested for flow cytometry analysis. Cells were stained for surface markers CD4 and CD69 for 20 min at room temperature before proceeding to intracellular marker staining (NFκB, Ki67, T-bet, IFN-γ, IL-2, GATA-3, IL-4, IL-13, RORγ, IL-17A, and FoxP3). For intracellular staining, BD Fixation/Permeabilization Solution Kit (BD Biosciences, Catalog # 555028) was used, as per the manufacturer's instructions. Antibody isotype controls were included. FlowJo Software (FlowJo, LLC) version 10.6.1 was used to analyze the data.

2.11. Th1/Th2/Th17 T-cell profiling by cytokine bead array

Human Th1/Th2/Th17 cytokine bead array (BD Biosciences, Catalog # 560484) was used to assess cytokine expression from CD4 + T-cells exposed to control and CSE-exposed iDC-EVs. Frozen CD4+ cells were thawed and washed once with serum-free medium, then cultured overnight in 10 % FBS containing medium. The following day, cells were pelleted and resuspended in fresh medium at a density of 20×10^6 cells/mL. 100 µL of cells and 100 µL resuspended EVs were mixed and cultured for two days in a 96-well plate. Conditioned medium was collected after pelleting the cells and stored at -80°C until use.

Th1/Th2/Th17 cytokine bead array (BD Biosciences, Catalog # 560484) was performed by following the manufacturer's protocol. Briefly, in a 1.5 mL Eppendorf tube, 50 µL of mixed Th1/Th2/Th17

cytokine capture beads were added to the tube, then 50 μL of two-fold serial diluted standard or cytokine-containing conditioned medium was added, followed by 50 μL of Th1/Th2/Th17 PE detection reagent. After mixing well, the tubes were incubated at room temperature for 3 h, protected from light. After the incubation, 1 mL washing buffer was added to each tube and centrifuged at 200 x g for 5 min. The supernatant in the tube then was carefully removed before adding 300 μL of Washing buffer to resuspend the sample pellet before FACS analysis. The final data analysis was done by using BD FCAP Array v1.0 software.

2.12. HIV infection

Previously isolated CD4 + T-cells were thawed from liquid nitrogen and cultured overnight in 10 % FBS, RPMI-1640 cell culture medium. Cells were harvested and washed once with serum-free medium and aliquoted in a 96-well plate (4×10^5 cells/well). Equal volumes of resuspended 100k UC pellets from unconditioned media, as well as control and CSE iDC-EVs, were added to corresponding wells and mixed thoroughly. After two days in culture, cells were harvested and washed once with serum-free medium. Cells were then infected with HIV.MN (200−400 ng p24/mL) for 4 h at 37 °C. Cells were washed twice with
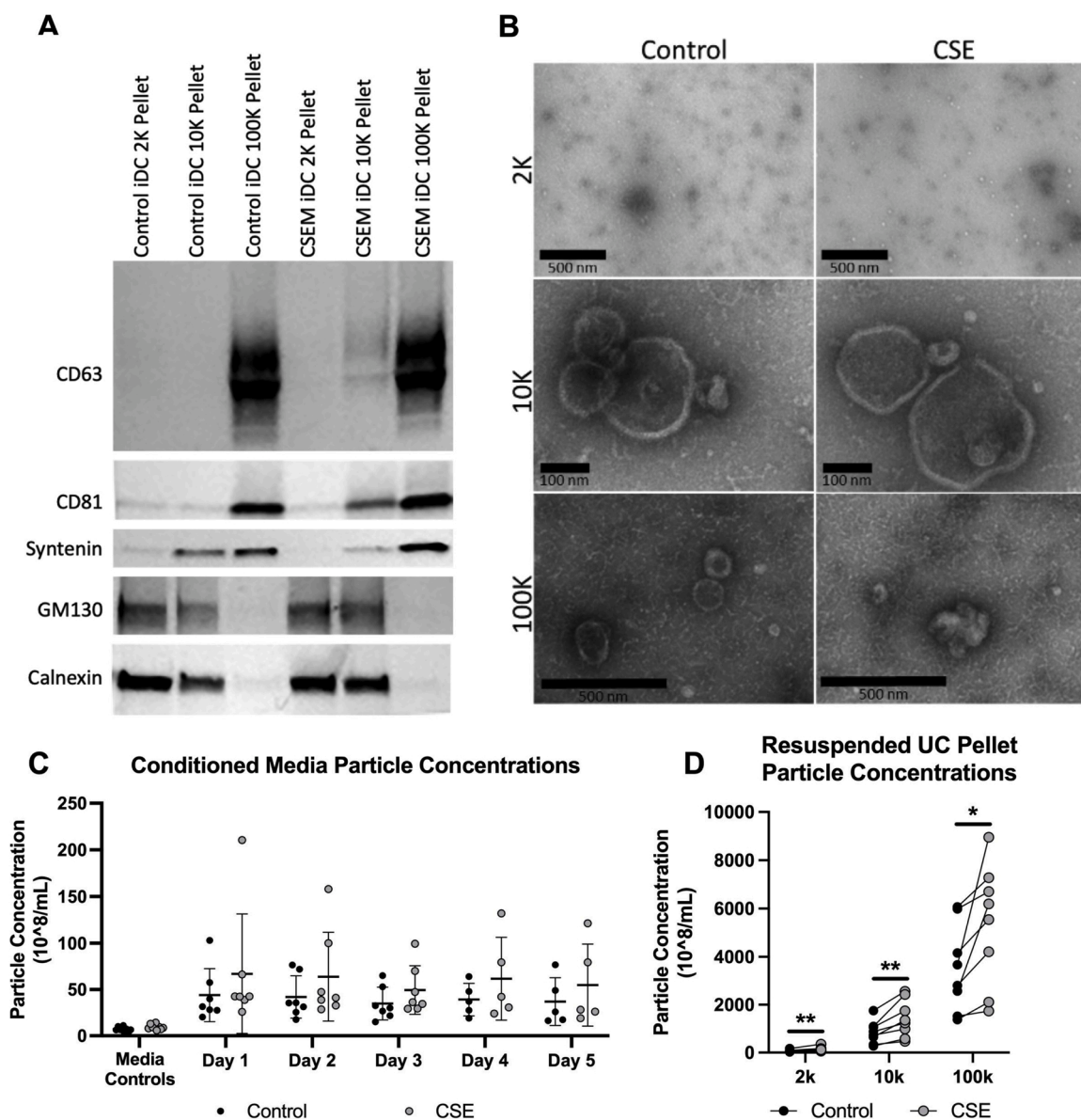

Fig. 1. Control and CSE-Induced iDC-EV Characterization. (A) Western blot analysis showed enrichment of CD63 the 100k pellet of both control and CSE sample preps, and minimal enrichment in the CSEM 10k pellet. CD81 and syntenin were observed in all sample preps, however expression of each was predominantly observed in the 100k pellets. Depletion of GM130 and reduced expression of Calnexin was observed in the 100k pellets. (B) Electron microscopy images of the 2k, 10k, and 100k pellets from control and CSE cell conditioned media demonstrate expected EV morphology. (C) Compared with unconditioned media, there were significantly more particles present in the control iDC conditioned media ($F_{5,39} = 3.758$, $p = 0.0081$). Dunnett's post-hoc analyses indicated that significantly more particles were counted in the conditioned media on day 1 ($p = 0.0045$), day 2 ($p = 0.0076$), day 3 ($p = 0.0446$), and day 4 ($p = 0.036$), with day 5 at $p = 0.0523$. Despite apparent higher numbers of particles, compared with unconditioned CSE media, there were no significant differences in particle concentrations in the CSE-exposed iDC conditioned media ($F_{5,39} = 2.157$, $p = 0.0822$), which is likely due to high variability of particle number in the CSE-conditioned media. (D) After performing differential ultracentrifugation, significantly more particles were counted in the CSE-exposed conditioned media than the AIM-V conditioned media controls in the 2k ($p = 0.009$), 10k ($p = 0.0046$), and 100k ($p = 0.0204$) resuspended UC pellets. Data are expressed as mean ± SD. Paired *t*-test; *p < 0.05, **p < 0.01.

serum-free medium and re-seeded in a new 96-well plate with the same condition as before infection. After three additional days in culture, cells were harvested and counted. Conditioned supernatant was lysed with 1% Triton X-100, and p24 concentration was measured by ELISA (Perkin Elmer, Catalog # NEK050B001KT) to quantify virus production, as per the manufacturer's instructions.

2.13. HIV latency: ACH-2 cells

ACH-2 cells (AIDS reagent #349) were used to study the effects of direct CSE exposure and iDC-EVs on HIV latency. To test the effects of CSE exposure, cells were cultured in 24-well plates and exposed daily to fresh RPMI-1640 cell culture media containing various concentrations of CSE (0, 50, 75, and 100 %) for 3 days. Conditioned media were collected from each well and centrifuged at 1000 x g for 5 min. Pelleted cells were resuspended in fresh medium containing 0, 50, 75, or 100 % CSE, and re-plated at a density of 1×10^6 cells per well. To test the effects of iDC-EVs, ACH-2 cells were seeded in a 96-well plate at a density of 5×10^4 cells per well in 100 μL volume. 100 μL of EVs (2k, 10k, or 100k resuspended pellets) were added to the cells, which were cultured for three days. At the conclusion of the exposure period, cells were pelleted, and conditioned supernatant was transferred to a fresh tube. Conditioned supernatant was lysed with 1% Triton X-100. p24 concentration was measured by ELISA (Perkin Elmer, Catalog # NEK050B001KT).

2.14. Statistical analyses

Statistically significant differences of particle concentrations in unconditioned media vs. iDC conditioned media for control and CSE exposed iDCs in Fig. 1C were analyzed by one-way ANOVA, followed by Dunnett's multiple comparison post-hoc tests. Significance was defined as corrected $p < 0.05$. Statistical significance of differences in total particle concentrations in Fig. 1D was assessed with paired t-tests for each resuspended UC pellet. Differences in protein expression on control vs. CSE iDC-EVs detected by the MACSPlex kit in Fig. 2 were analyzed with paired t-tests, and statistical significance was determined with Bonferroni corrections, with significance defined as $p < 0.0025$. Statistical differences in p24 release from ACH-2 cells exposed to varying concentrations of CSE across three days in Fig. 6B were assessed with a two-way ANOVA, followed by Dunnett's multiple comparison post-hoc tests, with significance defined as corrected $p < 0.05$.

2.15. Data availability and compliance

Data can be made available upon request to the corresponding author. For all experiments, we sought to achieve compliance with the International Society for Extracellular Vesicles recommendations for minimal information for studies of extracellular vesicles (Théry et al., 2018). We have submitted relevant experimental details to the EV-TRACK knowledgebase (EV-TRACK ID: EV200070) (Van Deun et al., 2017).

3. Results

3.1. EV characterization

To assess separation of EVs from iDC conditioned cell culture media, Western blot and electron microscopy were performed. Western blotting confirmed the presence of CD63 in the 100k pellet from both control and CSE-exposed iDCs, and CD81 and syntenin in all sample preps, with predominant enrichment in the 100k pellets (Fig. 1A). Depletion of the cis-Golgi matrix protein, GM130, and the endoplasmic reticulum protein, Calnexin, in the 100k pellets, indicate low amounts of intracellular contamination of the small EV pellets from both control and CSE-exposed iDCs (Fig. 1A). The 2k, 10k, and 100k pellets were visualized with TEM (Fig. 1B) with no obvious morphological differences between control and CSE iDC-EVs. Uncropped electron microscopy images are shown in Supplemental Fig. 1.

Particles in both unconditioned and iDC conditioned media from each day of culture were counted by nanoparticle tracking analysis (Fig. 1C). Relative to unconditioned media, significantly more particles were counted in the conditioned media of control iDCs on days 1–4, while no significant differences were observed between unconditioned CSE media and CSE-exposed iDC conditioned media (Fig. 1C). Next, media from all five days were pooled, and vesicles were partially separated by differential ultracentrifugation (Fig. 1D). Significantly more particles were detected in the resuspended UC pellets obtained from CSE-exposed iDCs than from control iDCs. Size distributions of particles from the 2k, 10k, and 100k pellets were not different for resuspended control and CSE UC pellets (Supplemental Fig. 2).

We next assessed the expression of thirty-six EV surface proteins on EVs bearing CD9/CD63 and/or CD81 using the MACSPlex Exosome kit. After normalizing each sample to total fluorescence, we found that, while control and CSE-EVs displayed similar levels of CD63 and CD9, the
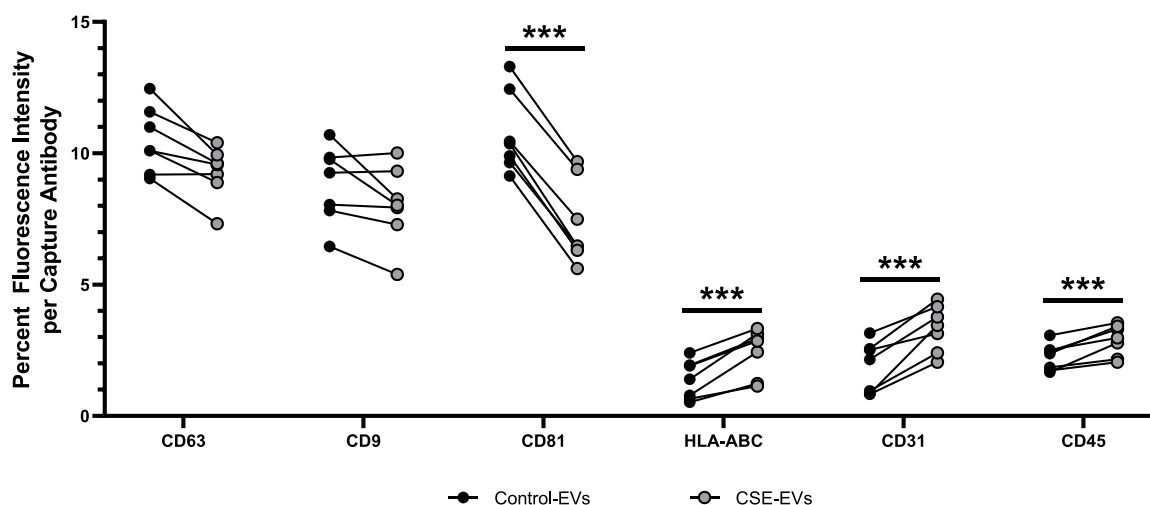

Fig. 2. EV Surface Markers. Percent fluorescence intensity per capture antibody indicate that there were no significant differences in expression of CD63 ($p = 0.0074$) or CD9 ($p = 0.073$) between control and CSE-EVs. Expression of CD81 was significantly lower ($p < 0.0001$) in the CSE-EVs compared with control EVs. Expression levels of HLA-ABC ($p = 0.0009$), CD31 ($p = 0.0009$), and CD45 ($p = 0.0024$) were all significantly upregulated in the CSE-EVs when compared with control EVs. Data are expressed as mean ± SD. Paired t-test with Bonferroni corrections; ***$p < 0.0025$.

EVs from CSE-exposed cells had significantly lower levels of CD81 (Fig. 2). Three markers (HLA-ABC, CD31, and CD45) were significantly upregulated on CSE-EVs versus control EVs. Markers that were not significantly different are shown in Supplemental Fig. 3.

3.2. T-cell activation by iDC-EVs

Because DC EVs have previously been shown to induce T-cell activation (Tkach et al., 2017), we were curious as to whether CSE-induced iDC-EVs may also impact T-cell activation and differentiation. Therefore, we sought to determine the effect of varying doses of iDC-CSE EVs from the 100k UC pellet on T-cell activation after one or two days of exposure to low, medium, and high doses of EVs. Due to the high variability of iDC yields from each Leukopak, there was also high variability in vesicle yields. We utilized roughly the same number of dendritic cells and volumes of separated EVs, and categorized them into "low", "medium" and "high" dose groups to account for this variability. Using flow cytometry, we assessed T-cell activation and Th1, Th2, and Th17 differentiation markers. RORγt and FoxP3 are key transcription factors for T-cell differentiation to either Th17 or Treg, respectively (Zhou et al., 2008). Both factors were upregulated after exposure to CSE-EVs in a dose-dependent fashion on day 1 and this effect was maintained on day 2 (Fig. 3A and B, respectively). The main effector cytokine of Th17 cells, IL-17A, was also upregulated across both days in a dose-dependent fashion (Fig. 3C). To a lesser extent, we also observed dose-dependent upregulation of Th1 transcription factor T-Bet across both days (Fig. 3D). IFN-γ, the main effector cytokine of Th1 cells, slightly decreased in response to exposure to control iDC-EVs in a dose-dependent fashion on day 1 and remained low regardless of dose on day 2 (Fig. 3E). Conversely, IFN-γ expression increased after exposure to the highest dose of iDC-CSE EVs on day 1, expression was reduced for all doses by day 2 (Fig. 3E). Dose-dependent increases of IL-2 were seen on both days after exposure to iDC-CSE EVs (Fig. 3F). For markers of T-cell activation and proliferation and Th2 differentiation, individual variability but no large, consistent effects were observed (Supplemental Fig. 4). Expression of the p65 subunit of NFκB (Supplemental Fig. 4A), a marker of activated T-cells, was not altered after exposure to iDC-CSE EVs on either day. The activation marker CD69 (Supplemental Fig. 4B) increased in a dose-dependent fashion in response to both types of EVs, but only for one donor. No changes in expression of the proliferation marker Ki67 were detected (Supplemental Fig. 4C). The Th2 transcription factor, GATA-3 (Supplemental Fig. 4D), showed large changes in expression after exposure to the medium iDC-CSE EV dose in several donors on day 1, but this effect was attenuated by day 2.

Expression of the two main effector cytokines of Th2 cells, IL-4 (Supplemental Fig. 4E) and IL-13 (Supplemental Fig. 4F), was not altered by either control or CSE iDC-EVs after one day of exposure.

3.3. Th1/Th2/Th17 cytokine bead array

Autologous T-cells from three donors (Leukopaks) were exposed to a "high" dose of resuspended control or CSE 2k, 10k, and 100k pellets for 24 h and conditioned cell culture media were collected. Cytokine bead array revealed heterogeneous responses that varied greatly by donor (Fig. 4). Increased expression of TNF-α and IL-6, markers of Th1 and Th2 differentiation, respectively, was observed for Leukopak 13, especially when exposed to the 100 K CSE EV pellet (Fig. 4A). T-cells from Leukopak 16 also demonstrated increased secretion of TNF-α and IL-6, as well as IFN-γ (another Th1 marker), when exposed to the 100 K CSE pellet (Fig. 4B). Conversely, T-cells from Leukopak 21 (Fig. 4C) showed increased expression of TNF-α only after exposure to the 10k CSE pellet, but decreased secretion of TNF-α after exposure to the 2k CSE pellet. Leukopak 21 also showed decreased expression of IFN-γ, IL-10, IL-4, and IL-6 after exposure to various EV pellets (Fig. 4C).

3.4. p24 release is not significantly affected by iDC-EVs or direct CSE exposure

To determine the effects of iDC-EVs on HIV infection, CD4 + T cells were infected with HIV and then exposed to different doses of resuspended 100k UC pellets of either unconditioned AIM-V or CSE media, or control or CSE iDC-EVs (Fig. 5). Despite differences across Leukopaks, a trend could be observed: cells infected with HIV and then exposed to either control or CSE iDC-EVs supported less p24 release, indicative of reduced virus replication. We next assessed the effects of iDC-CSE EVs on ACH-2 p24 release after 3 days of exposure (Fig. 6 A). Interestingly, the 2k UC pellet of iDC-EVs slightly increased p24 release from ACH-2 cells after exposure to both control and CSE-derived EVs. The 10k and 100k UC pellets had no strong effect on p24 release. We next assessed p24 release from ACH-2 cells after direct CSE exposure for three successive days (Fig. 6B). We observed a statistically significant interaction between day of CSE exposure and CSE concentration (p = 0.0124). We observed a statistically significant main effect of day of exposure (p < 0.0001) as well. Dunnett's multiple comparison post-hoc analyses showed significant differences on day 1 between 0 and 50 % CSE (p = 0.0373), and on day 2 between 0 and 75 % CSE (p = 0.004), with CSE exposure inducing more p24 release. On day 3, there was a significant difference in p24 release between 0 and 100 % CSE exposure; however,
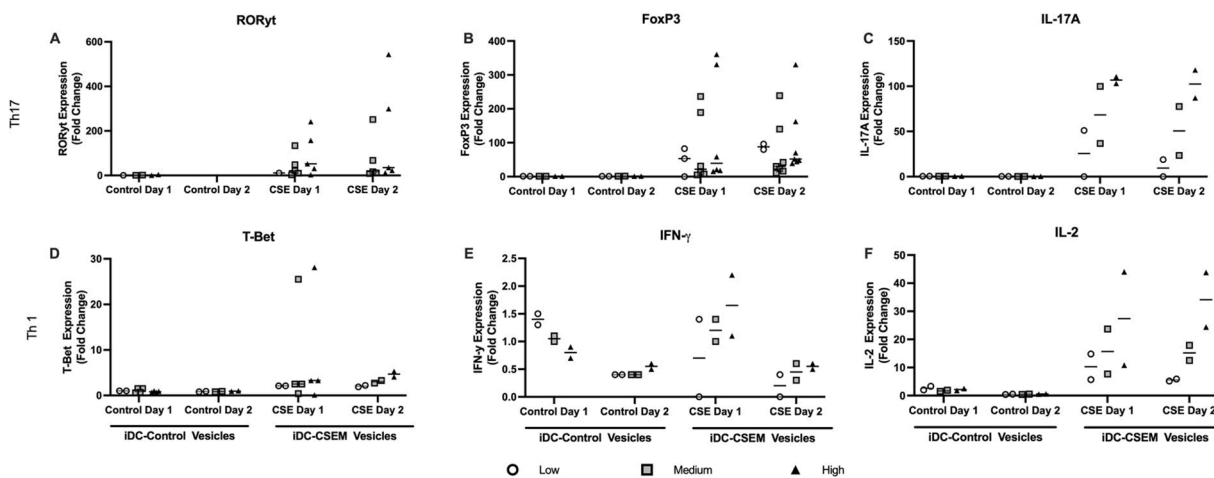

Fig. 3. iDC-CSE EVs induce expression of Th17 and Th1 differentiation markers. FACS analysis of Th17 transcription factors (A, B) and main effector cytokine (C) and Th1 transcription factor (D) and effector cytokine (F) show increased expression after both 1 and 2 days of exposure to CSE-induced iDC-EVs, except for the Th1 effector cytokine, IFN-γ, which only showed increased expression on day 1 of exposure.
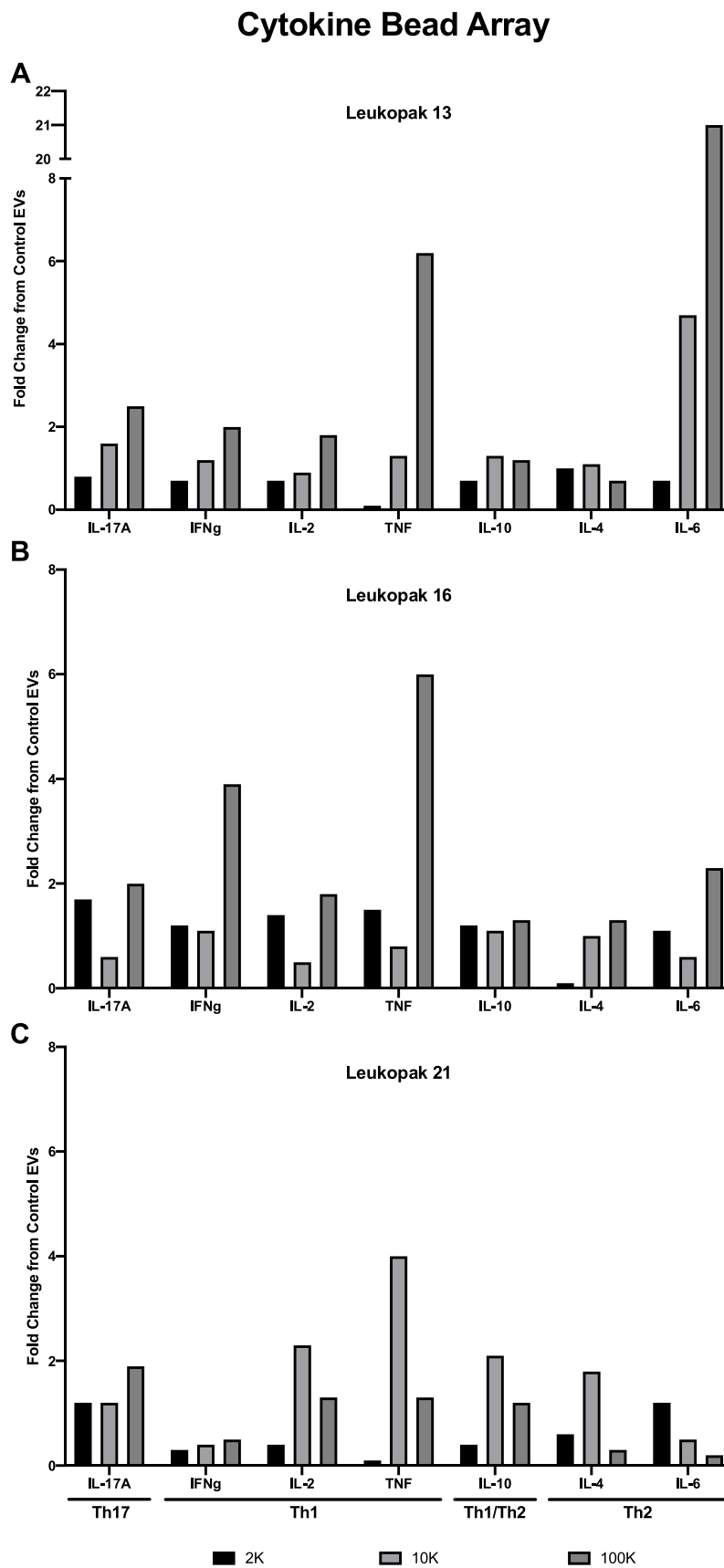
Cytokine Bead Array

Fig. 4. Th1/Th2/Th17 Cytokine bead array. Cytokine secretion from autologous T-cells after exposure to resuspended control and CSE EV 2k, 10k, and 100k pellets. Leukopak 13 (A) and Leukopak 16 (B) showed increased expression of TNF-α after exposure to the 100k CSE EVs. Leukopak 13 (A) also showed increased secretion of IL-6, while Leukopak 16 (B) showed increased expression of IFN-γ. Leukopak 21 (C) demonstrated reduced secretion of several cytokines after exposure to CSE EVs.
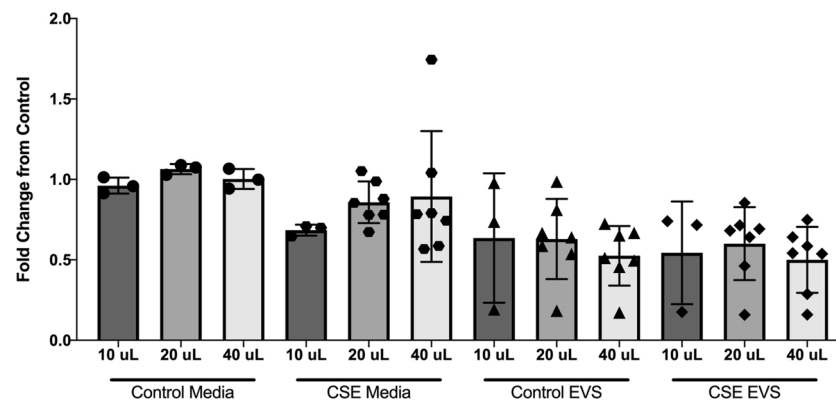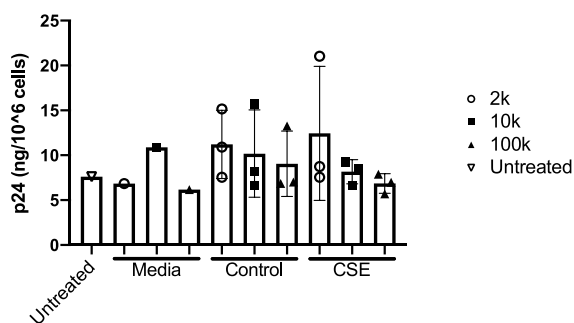
Fig. 5. p24 release from HIV-infected primary CD4 + T cells. CD4 + T cells were infected with HIV and exposed to varying volumes of resuspended 100k UC pellets of either unconditioned media or iDC-EVs. Exposure to iDC-EVs (control or CSE) reduced p24 release relative to controls and unconditioned media UC pellets, at 10, 20, and 40 μL volumes from most donors.
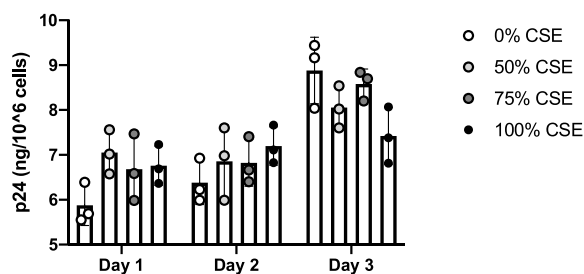

Fig. 6. HIV-containing ACH-2 cells were directly exposed to varying concentrations of CSE; there were no significant effects on p24 release (A). ACH-2 cells were also exposed to iDC-EVs, and p24 release was assessed after 24 h (B).

less p24 was released from the CSE exposed cells on this day. Here, we find that CSE exposure increased p24 release relative to controls on days 1 and 2, but by day 3, p24 release was higher in the control group than the CSE exposed cells.

4. Discussion

EVs serve as nano-sized intercellular communicators and have been shown to participate in immune responses, especially by activating T-cells (reviewed by Robbins and Morelli, 2014). Previous work has demonstrated the ability of B-cell-derived EVs to activate T-cells (Muntasell et al., 2007) and that activated T-cells can release EVs expressing MHC-I molecules (Blanchard et al., 2002). Others have shown that DC-derived EVs have the capacity to activate naïve T-cells (Buschow et al., 2009; Nolte-'t Hoen et al., 2009). In the current study,

we examined the effects of CSE on EV release from primary iDCs and how these EVs affected CD4 + T-cell activation and HIV infection.

Although we did not observe any morphological differences in EVs released from control or CSE-exposed iDCs (Fig. 1B), significantly more particles were counted in the CSE-exposed iDC 2k, 10k, and 100k UC pellets when compared with the corresponding control iDC UC pellets (Fig. 1D). Control iDC conditioned media contained significantly more particles than unconditioned control media, whereas particle counts from CSE-exposed iDC conditioned media did not significantly differ from unconditioned CSE media (Fig. 1C). Together, these data suggest that there may be more NTA-detected particulates in the CSE media than in control media. However, since ultracentrifugation is not specific to EVs, it is possible that non-EV particulates contribute to or account for this difference.

It is important to note that loading of EV samples for Western blotting was based on re-suspended UC pellet volumes, whereas loading of EV samples for the MACSPlex Exosome assay was based on normalized particle counts. Western blotting revealed more intense banding for CD63, CD81, and syntenin in the 100k CSE pellet compared with the 100k control pellet (Fig. 1A); indeed, our NTA data indicate that there are significantly more particles present in the 100k CSE pellet compared with the 100k control pellet (Fig. 1D). Conversely, data from the MACSPlex assay show no significant difference in CD63 expression between control and CSE 100k pellets, whereas expression of CD81 is significantly lower in the CSE 100k pellet compared with the control 100k pellet (Fig. 2). Therefore, our data suggest that after controlling for particle concentration, there are no differences in CD63 expression between control and CSE-EVs, but that CSE-EVs express significantly lower levels of CD81 than control EVs. Previous research has shown that the activation of smoking-related inflammatory pathways downregulates CD81 and CD9 expression in a macrophage cell line (Takeda et al., 2008). Although CD9 was not significantly downregulated, there was a downward trend in its expression in CSE-EVs relative to control EVs (Fig. 2). As circulating CD14+ monocytes can be differentiated into both macrophages and dendritic cells, it is plausible that these iDCs would have similar behaviors to macrophages and would result in downregulation of CD81 and CD9 post-CSE exposure. Cigarette smoking has also been shown to alter EV profiles in humans (Wu et al., 2019); an alternative explanation for these data is that CSE exposure alters intracellular signaling pathways in a way that affects EV formation and/or release (Reviewed by Ryu et al., 2018).

EV phenotyping data also suggest that EV displays of HLA-ABC, CD31, and CD45 are significantly altered in response to CSE exposure (Fig. 2). HLA-ABC are MHC-class I molecules that play an important role in regulating the immune response by presenting antigens to CD8+ T-cells. Here, we find that after cigarette exposure, EVs released from iDCs express significantly higher levels of HLA-ABC than control EVs.

Previous work in macrophages demonstrated that cigarette exposure downregulates MHC-class I expression (Kammerl et al., 2016); this phenomenon occurs in cancer cells as they downregulate expression of HLA molecules to prevent ingestion and destruction by cytotoxic CD8+ T-cells (Chaganty et al., 2016). In the current study we did not assess cellular expression of HLA-ABC after CSE exposure; this may be an interesting avenue for future research to better understand how cigarette smoke modulates iDC intracellular signaling pathways and why we observe increased HLA expression in released EVs. CD31 is an endothelial cell adhesion molecule that is also present on platelets and leukocytes, and although its exact mechanisms have not yet been fully elucidated, is thought to play a role in suppressing T-cell activation (Liu and Shi, 2012; Marelli-Berg et al., 2013). Previous work using endothelial cells showed that after CSE exposure, CD31 expression was increased (Soghomonians et al., 2004). Similarly, e-cigarette smoke increased CD31 expression in murine cardiac tissue (Shi et al., 2019). CD45 is a transmembrane phosphotyrosine phosphatase ubiquitously expressed in all leukocytes and has previously been shown to be upregulated on EVs isolated from platelets and leukocytes after CSE exposure (Mobarrez et al., 2014). CD45 is likely required for T-cell activation via the T-cell receptor (Altin and Sloan, 1997). While increased expression of HLA-ABC and CD45 on CSE-EVs may have worked towards activating T-cells, the suppressive effects of CD31 signaling may have reduced T-cell activation; together these data may explain why we did not see large increases in the expression of markers of T-cell activation (Supplemental Fig. 4).

Differentiation of cells from a Th0 phenotype to either Th1 or Th2 is dependent on the cytokine environment (Zhu et al., 2010). Th0 cells secrete IFN-y, IL-2, and IL-4 and the proportions of each cytokine will drive differentiation towards Th1 or Th2 subtypes. As cells continue to differentiate, they begin to secrete major effector cytokines of their specific subtype, which can inhibit differentiation of the other subtype. For example, Th1 differentiation is driven by IFN-y, prompting cells to secrete more IFN-y, which inhibits Th2 differentiation. After exposure to CSE-EVs, we observed increased expression in the key Th1 transcription factor T-Bet concurrent with production of IFN-y and IL-2 (Fig. 3D, E, F). Although cells from some donors showed an increase in expression of the Th2 transcription factor, GATA-3, expression of the main effector cytokines of the Th2 response, IL-4 and IL-13, was not markedly changed (Supplemental Fig. 4D, E, F). In addition, we also observed increased expression of markers indicative of Th17 differentiation (Fig. 3A, B, C). Th17 cells have been shown to play major roles in the immune responses of a number of human diseases, including respiratory diseases like asthma and chronic obstructive pulmonary disorder (Tesmer et al., 2008). Previous work has shown that cigarette smoke exposure promotes differentiation of CD4 + T cells to Th17 cells, both *in vivo* and *in vitro* (Liang et al., 2018; Kim et al., 2019; Baskara et al., 2020), and that even post-cessation of cigarette use, Th17 and other inflammatory cells remain present at elevated levels in the lung (Duan et al., 2013). Our cytokine bead array data also suggest that, after CSE-EV exposure, CD4 + T-cells begin to differentiate towards the Th1 lineage, with the exception of one donor (Leukopak 13) who showed a very large increase in expression of IL-6, a pleiotropic cytokine that under certain conditions may push CD4 + T-cells towards Th2 differentiation (Rincón et al., 1997) (Fig. 4). These data further highlight the large amounts of individual variability observed in our studies using primary cells from several donors. Although we did not see evidence for Th17 differentiation in the cytokine bead array (Fig. 4) to the same extent as we did by flow cytometry (Fig. 3), it is important to note that samples from different donors were used across assays. Only one aspect of Th17 differentiation was assessed in the cytokine bead array (IL-17 production) compared with our flow cytometry assay, which also assessed expression of transcription factors indicative of Th17 differentiation. In addition, there are conflicting reports showing that differentiation of CD4 + T-cells to Th1 or Th17 can be antagonistic of one another (Luger et al., 2008), cooperative (O'Connor et al., 2008), or that phenotyping

switching from Th17 to Th1 can occur (Shi et al., 2008). In line with our findings, previous work has found that CSE exposure guides T-cells towards Th1 and Th17 pro-inflammatory phenotypes (Zhang et al., 2014).

Interestingly, we have also found that during acute HIV infection, autologous T cell exposure to CSE-induced iDC-EVs substantially reduces p24 production in most donors (Fig. 5). Conversely, previous work has described increased p24 release from macrophages exposed to cigarette smoke (Abbud et al., 1995; Ande et al., 2015). Using a latent HIV infected T cell line (ACH-2) we did not observe any major effects of either iDC-CSE EVs or direct CSE exposure on p24 release (Fig. 6), although p24 was slightly increased when cells were exposed directly to CSE (Fig. 6B). These findings may be more representative of HIV infected individuals with latent virus.

Of great importance is the substantial degree of individual differences (from one Leukopak to another) in our data. One explanation for these observations is that we have no information about the health or smoking status of the Leukopak donors. Cells isolated from donors who are current or past smokers may respond differently than cells from donors who have never smoked. Recent infections may also impact the functionality of the immune cells isolated from these Leukopaks, as well as medications the donors may be taking but are not required to disclose. Overall, our data suggest that CSE exposure alters EV production from dendritic cells, and these CSE-EVs can push T-cell differentiation towards Th17 and Th1 lineages. Future experiments will be needed to assess effects of variables such as age, sex, last known date of viral or bacterial infection, diagnosis of any chronic diseases, and recent medication taken prior to blood donation. Additionally, it would be useful to assess the effects of cigarette smoke with primary cells from patients infected with HIV.

Declaration of Competing Interest

The authors declare that they have no known competing financial interests or personal relationships that could have appeared to influence the work reported in this paper.

Acknowledgements

Appendix A. Supplementary data

Supplementary material related to this article can be found, in the online version, at doi:https://doi.org/10.1016/j.toxlet.2022.02.004.

References

Abbud, R.A., Finegan, C.K., Guay, L.A., Rich, E.A., 1995. Enhanced production of human immunodeficiency virus type 1 by in vitro-infected alveolar macrophages from otherwise healthy cigarette smokers. J. Infect. Dis. 172, 859–863. Available at: http://www.ncbi.nlm.nih.gov/pubmed/7658083 (Accessed March 19, 2020).

Altin, J.G., Sloan, E.K., 1997. The role of CD45 and CD45-associated molecules in T cell activation. Immunol. Cell Biol. 75, 430–445. Available at: https://pubmed.ncbi.nlm.nih.gov/9429890/ (Accessed July 15, 2020).

Ande, A., McArthur, C., Ayuk, L., Awasom, C., Achu, P.N., Njinda, A., Sinha, N., Rao, P.S. S., Agudelo, M., Nookala, A.R., Simon, S., Kumar, A., Kumar, S., 2015. Effect of mild-to-moderate smoking on viral load, cytokines, oxidative stress, and cytochrome P450 enzymes in HIV-infected individuals. PLoS One 10.

Baskara, I., Kerbrat, S., Dagouassat, M., Nguyen, H.Q., Guillot-Delost, M., Surenaud, M., Baillou, C., Lemoine, F.M., Morin, D., Boczkowski, J., Le Gouvello, S., 2020. Cigarette smoking induces human CCR6+Th17 lymphocytes senescence and VEGF-A secretion. Sci. Rep. 10, 1–11. Available at: https://doi.org/10.1038/s41598-020-63613-4 (Accessed July 16, 2020).

Bernstein, E.D., Liao, Z., Witwer, K.W., 2019. Cytotoxicity of aqueous cigarette smoke extract is affected by properties of pipettes used to prepare the extract. Matters 2019. Available at: http://www.ncbi.nlm.nih.gov/pubmed/32104671 (Accessed June 17, 2020).

Blanchard, N., Lankar, D., Faure, F., Regnault, A., Dumont, C., Raposo, G., Hivroz, C., 2002. TCR activation of human t cells induces the production of exosomes bearing

the TCR/CD3/ζ complex. J. Immunol. 168, 3235–3241. Available at: https://pubmed.ncbi.nlm.nih.gov/11907077/ (Accessed July 17, 2020).

Bleul, C.C., Wu, L., Hoxie, J.A., Springer, T.A., Mackay, C.R., 1997. The HIV coreceptors CXCR4 and CCR5 are differentially expressed and regulated on human T lymphocytes. Proc. Natl. Acad. Sci. U. S. A. 94, 1925–1930.

Buschow, S.I., Nolte-'t Hoen, E.N., van Niel, G., Pols, M.S., ten Broeke, T., Lauwen, M., Ossendorp, F., Melief, C.J., Raposo, G., Wubbolts, R., Wauben, M.H., Stoorvogel, W., 2009. MHC II in dendritic cells is targeted to lysosomes or T cell-induced exosomes via distinct multivesicular body pathways. Traffic 10, 1528–1542.

Chaganty, B.K.R., Lu, Y., Qiu, S., Somanchi, S.S., Lee, D.A., Fan, Z., 2016. Trastuzumab upregulates expression of HLA-ABC and T cell costimulatory molecules through engagement of natural killer cells and stimulation of IFNγ secretion. Oncoimmunology 5. Available at: /pmc/articles/PMC4839349/?report=abstract (Accessed July 15, 2020).

Chinnapaiyan, S., Unwalla, H.J., 2015. Mucociliary dysfunction in HIV and smoked substance abuse. Front. Microbiol. 6. Available at: https://pubmed.ncbi.nlm.nih.gov/26528246/ (Accessed July 16, 2020).

Chinnapaiyan, S., Dutta, R., Bala, J., Parira, T., Agudelo, M., Nair, M., Unwalla, H.J., 2018. Cigarette smoke promotes HIV infection of primary bronchial epithelium and additively suppresses CFTR function. Sci. Rep. 8, 1–10. Available at: www.nature.com/scientificreports (Accessed July 16, 2020).

Cozen, W., Diaz-Sanchez, D., Gauderman, W.J., Zadnick, J., Cockburn, M.G., Gill, P.S., Masood, R., Hamilton, A.S., Jyrala, M., Mack, T.M., 2004. Th1 and Th2 cytokines and IgE levels in identical twins with varying levels of cigarette consumption. J. Clin. Immunol. 24, 617–622.

Creamer, M.L.R., Wang, T.W., Babb, S., Cullen, K.A., Day, H., Willis, G., Jamal, A., Neff, L., 2019. Tobacco product use and cessation indicators among adults - United States, 2018. MMWR Morb. Mortal. Wkly. Rep. 68, 1013–1019. Available at: http://www.ncbi.nlm.nih.gov/pubmed/31725711 (Accessed February 24, 2020).

Diaz, P.T., King, M.A., Pacht, E.R., Wewers, M.D., Gadek, J.E., Neal, D., Nagaraja, H.N., Drake, J., Clanton, T.L., 1999. The pathophysiology of pulmonary diffusion impairment in human immunodeficiency virus infection. Am. J. Respir. Crit. Care Med. 160, 272–277. Available at: http://www.atsjournals.org/doi/abs/10.1164/ajrccm.160.1.9812089 (Accessed July 16, 2020).

Duan, M.-C., Tang, H.-J., Zhong, X.-N., Huang, Y., 2013. Persistence of Th17/Tc17 cell expression upon smoking cessation in mice with cigarette smoke-induced emphysema. Clin. Dev. Immunol. 2013, 11. Available at: http://dx. (Accessed July 16, 2020).

Feigin, V.L., et al., 2014. Global and regional burden of stroke during 1990-2010: findings from the Global Burden of Disease Study 2010. Lancet (London, England) 383, 245–254. Available at: http://www.ncbi.nlm.nih.gov/pubmed/24449944 (Accessed December 16, 2018).

Harrison, S.C., 2008. Viral membrane fusion. Nat. Struct. Mol. Biol. 15, 690–698. Available at: http://www.ncbi.nlm.nih.gov/pubmed/18596815 (Accessed February 18, 2019).

Kammerl, I.E., et al., 2016. Impairment of immunoproteasome function by cigarette smoke and in chronic obstructive pulmonary disease. Am. J. Respir. Crit. Care Med. 193, 1230–1241. Available at: http://imagej.nih. (Accessed July 14, 2020).

Kim, M., Gu, B., Madison, M.C., Song, H.W., Norwood, K., Hill, A.A., Wu, W.J., Corry, D., Kheradmand, F., Diehl, G.E., 2019. Cigarette smoke induces intestinal inflammation via a Th17 cell-neutrophil axis. Front. Immunol. 10.

Le Rouzic, O., Koné, B., Kluza, J., Marchetti, P., Hennegrave, F., Olivier, C., Kervoaze, G., Vilain, E., Mordacq, C., Just, N., Perez, T., Bautin, N., Pichavant, M., Gosset, P., 2016. Cigarette smoke alters the ability of human dendritic cells to promote anti-Streptococcus pneumoniae Th17 response. Respir. Res. 17, 1.

Lee, J., Taneja, V., Vassallo, R., 2012. Cigarette smoking and inflammation: cellular and molecular mechanisms. J. Dent. Res. 91, 142–149.

Liang, Y., Shen, Y., Kuang, L., Zhou, G., Zhang, L., Zhong, X., Zhang, J., Liu, J., 2018. Cigarette smoke exposure promotes differentiation of CD4+ T cells toward Th17 cells by CD40-CD40L costimulatory pathway in mice. Int. J. COPD 13, 959–968.

Liao, Z., Muth, D.C., Eitan, E., Travers, M., Learman, L.N., Lehrmann, E., Witwer, K.W., 2017. Serum extracellular vesicle depletion processes affect release and infectivity of HIV-1 in culture. Sci. Rep. 7.

Liu, L., Shi, G.-P., 2012. CD31: Beyond a Marker for Endothelial Cells. Available at: https://academic.oup.com/cardiovascres/article-abstract/94/1/3/272760 (Accessed July 15, 2020).

Luger, D., Silver, P.B., Tang, J., Cua, D., Chen, Z., Iwakura, Y., Bowman, E.P., Sgambellone, N.M., Chan, C.C., Caspi, R.R., 2008. Either a Th17 or a Th1 effector response can drive autoimmunity: conditions of disease induction affect dominant effector category. J. Exp. Med. 205, 799–810. Available at: https://pubmed.ncbi.nlm.nih.gov/18391061/ (Accessed July 16, 2020).

Manches, O., Frleta, D., Bhardwaj, N., 2014. Dendritic cells in progression and pathology of HIV infection. Trends Immunol. 35, 114–122.

Marelli-Berg, F.M., Clement, M., Mauro, C., Caligiuri, G., 2013. An immunologist's guide to CD31 function in T-cells. J. Cell. Sci. 126, 2343–2352. Available at: https://jcs.biologists.org/content/126/11/2343 (Accessed July 15, 2020).

Mobarrez, F., Antoniewicz, L., Bosson, J.A., Kuhl, J., Pisetsky, D.S., Lundbäck, M., 2014. The effects of smoking on levels of endothelial progenitor cells and microparticles in the blood of healthy volunteers. PLoS One 9. Available at: /pmc/articles/PMC3938677/?report=abstract (Accessed July 15, 2020).

Muntasell, A., Berger, A.C., Roche, P.A., 2007. T cell-induced secretion of MHC class II-peptide complexes on B cell exosomes. EMBO J. 26, 4263–4272. Available at: /pmc/articles/PMC2230838/?report=abstract (Accessed July 17, 2020).

Nolte-'t Hoen, E.N.M., Buschow, S.I., Anderton, S.M., Stoorvogel, W., Wauben, M.H.M., 2009. Activated T cells recruit exosomes secreted by dendritic cells via LFA-1. Blood

113, 1977–1981. Available at: https://pubmed.ncbi.nlm.nih.gov/19064723/ (Accessed July 17, 2020).

O'Connor, R.A., Prendergast, C.T., Sabatos, C.A., Lau, C.W.Z., Leech, M.D., Wraith, D.C., Anderton, S.M., 2008. Cutting edge: Th1 cells facilitate the entry of Th17 cells to the central nervous system during experimental autoimmune encephalomyelitis. J. Immunol. 181, 3750–3754. Available at: https://pubmed.ncbi.nlm.nih.gov/18768826/ (Accessed July 16, 2020).

Onor, I.C.O., Stirling, D.L., Williams, S.R., Bediako, D., Borghol, A., Harris, M.B., Darensburg, T.B., Clay, S.D., Okpechi, S.C., Sarpong, D.F., 2017. Clinical effects of cigarette smoking: epidemiologic impact and review of pharmacotherapy options. Int. J. Environ. Res. Public Health 14. Available at: http://www.ncbi.nlm.nih.gov/pubmed/28956852 (Accessed February 24, 2020).

Qiu, F., Liang, C.L., Liu, H., Zeng, Y.Q., Hou, S., Huang, S., Lai, X., Dai, Z., 2017. Impacts of cigarette smoking on immune responsiveness: Up and down or upside down? Oncotarget 8, 268–284.

Rao, P., Anusha, A., Sinha, N., Kumar, A., Kumar, S., 2016. Effects of cigarette smoke condensate on oxidative stress, apoptotic cell death, and HIV replication in human monocytic cells. PLoS One 11. Available at: https://pubmed.ncbi.nlm.nih.gov/27203850/ (Accessed July 16, 2020).

Reynolds, N.R., 2009. Cigarette smoking and HIV: more evidence for action. AIDS Education and Prevention. AIDS Educ Prev., pp. 106–121

Rincón, M., Anguita, J., Nakamura, T., Fikrig, E., Flavell, R.A., 1997. Interleukin (IL)-6 directs the differentiation of IL-4-producing CD4+ T cells. J. Exp. Med. 185, 461–469. Available at: https://pubmed.ncbi.nlm.nih.gov/9053446/ (Accessed October 2, 2020).

Robbins, P.D., Morelli, A.E., 2014. Regulation of immune responses by extracellular vesicles. Nat. Rev. Immunol. 14, 195–208.

Robbins, C.S., Franco, F., Mouded, M., Cernadas, M., Shapiro, S.D., 2008. Cigarette smoke exposure impairs dendritic cell maturation and t cell proliferation in thoracic lymph nodes of mice. J. Immunol. 180, 6623–6628.

Ryu, A.-R., Kim, D.H., Kim, E., Lee, M.Y., 2018. The potential roles of extracellular vesicles in cigarette smoke-associated diseases. Oxid. Med. Cell. Longev. Available at: https://doi.org/10.1155/2018/4692081 (Accessed July 14, 2020).

Shi, G., Cox, C.A., Vistica, B.P., Tan, C., Wawrousek, E.F., Gery, I., 2008. Phenotype switching by inflammation-inducing polarized Th17 cells, but not by Th1 cells. J. Immunol. 181, 7205–7213. Available at: https://pubmed.ncbi.nlm.nih.gov/18981142/ (Accessed July 16, 2020).

Shi, H., Fan, X., Horton, A., Haller, S.T., Kennedy, D.J., Schiefer, I.T., Dworkin, L., Cooper, C.J., Tian, J., 2019. The effect of electronic-cigarette vaping on cardiac function and angiogenesis in mice. Sci. Rep. 9, 1–9. Available at: www.nature.com/scientificreports (Accessed July 15, 2020).

Soghomonians, A., Thirkill, T.L., Mariano, N.F., Barakat, A.I., Douglas, G.C., 2004. Effect of aqueous tobacco smoke extract and shear stress on PECAM-1 expression and cell motility in human uterine endothelial cells. Toxicol. Sci. 81, 408–418.

Sopori, M.L., Kozak, W., 1998. Immunomodulatory effects of cigarette smoke. J. Neuroimmunol. 83, 148–156.

Strzelak, A., Ratajczak, A., Adamiec, A., Feleszko, W., 2018. Tobacco smoke induces and alters immune responses in the lung triggering inflammation, allergy, asthma and other lung diseases: a mechanistic review. Int. J. Environ. Res. Public Health 15.

Takeda, Y., He, P., Tachibana, I., Zhou, B., Miyado, K., Kaneko, H., Suzuki, M., Minami, S., Iwasaki, T., Goya, S., Kijima, T., Kumagai, T., Yoshida, M., Osaki, T., Komori, T., Mekada, E., Kawase, I., 2008. Double deficiency of tetraspanins CD9 and CD81 alters cell motility and protease production of macrophages and causes chronic obstructive pulmonary disease-like phenotype in mice. J. Biol. Chem. 283, 26089–26097. Available at: http://www.jbc.org (Accessed July 14, 2020).

Talhout, R., Schulz, T., Florek, E., van Benthem, J., Wester, P., Opperhuizen, A., 2011. Hazardous compounds in tobacco smoke. Int. J. Environ. Res. Public Health 8, 613–628. Available at: http://www.ncbi.nlm.nih.gov/pubmed/21556207 (Accessed February 24, 2020).

Tesmer, L.A., Lundy, S.K., Sarkar, S., Fox, D.A., 2008. Th17 cells in human disease. Immunol. Rev. 223, 87–113. Available at: /pmc/articles/PMC3299089/?report=abstract (Accessed July 16, 2020).

Théry, C., et al., 2018. Minimal information for studies of extracellular vesicles 2018 (MISEV2018): a position statement of the International Society for Extracellular Vesicles and update of the MISEV2014 guidelines. J. Extracell. Vesicles 7, 1535750. Available at: https://www.tandfonline.com/doi/full/10.1080/20013078.2018.1535750 (Accessed January 6, 2019).

Tkach, M., Kowal, J., Zucchetti, A.E., Enserink, L., Jouve, M., Lankar, D., Saitakis, M., Martin-Jaular, L., Théry, C., 2017. Qualitative differences in T-cell activation by dendritic cell-derived extracellular vesicle subtypes. EMBO J. 36, 3012–3028. Available at: https://onlinelibrary.wiley.com/doi/abs/10.15252/embj.201696003 (Accessed October 2, 2020).

Tollerud, D.J., Clark, J.W., Brown, L.M., Neuland, C.Y., Mann, D.L., Pankiw-Trost, L.K., Blattner, W.A., Hoover, R.N., 1989. The Effects of Cigarette Smoking on T Cell Subsets: A Population-based Survey of Healthy Caucasians. https://doi.org/10.1164/ajrccm/13961446139.

Torres de Heens, G.L., van der Velden, U., Loos, B.G., 2009. Cigarette smoking enhances T cell activation and a Th2 immune response; an aspect of the pathophysiology in periodontal disease. Cytokine 47, 157–161.

Van Deun, J., et al., 2017. EV-TRACK: transparent reporting and centralizing knowledge in extracellular vesicle research. Nat. Methods 14, 228–232. Available at: http://www.ncbi.nlm.nih.gov/pubmed/28245209 (Accessed February 18, 2019).

Van Hove, C.L., Moerloose, K., Maes, T., Joos, G.F., Tournoy, K.G., 2008. Cigarette smoke enhances Th-2 driven airway inflammation and delays inhalational tolerance. Respir. Res. 9.

Vargas-Rojas, M.I., Ramírez-Venegas, A., Limón-Camacho, L., Ochoa, L., Hernández-Zenteno, R., Sansores, R.H., 2011. Increase of Th17 cells in peripheral blood of patients with chronic obstructive pulmonary disease. Respir. Med. 105, 1648–1654.

Vassallo, R., Tamada, K., Lau, J.S., Kroening, P.R., Chen, L., 2005. Cigarette smoke extract suppresses human dendritic cell function leading to preferential induction of Th-2 priming. J. Immunol. 175, 2684–2691.

Vijayaraghavan, M., Penko, J., Vittinghoff, E., Bangsberg, D.R., Miaskowski, C., Kushel, M.B., 2014. Smoking behaviors in a community-based cohort of HIV-infected indigent adults. AIDS Behav. 18, 535–543.

Wang, F., He, B., 2012. CCR1 and CCR5 expression on inflammatory cells is related to cigarette smoking and chronic obstructive pulmonary disease severity. Chin. Med. J. (Engl.) 125, 4277–4282. Available at: http://www.ncbi.nlm.nih.gov/pubmed/23217400 (Accessed March 18, 2020).

Wu, F., Yin, Z., Yang, L., Fan, J., Xu, J., Jin, Y., Yu, J., Zhang, D., Yang, G., 2019. Smoking induced extracellular vesicles release and their distinct properties in non-small cell lung cancer. J. Cancer 10. Available at: http://www.jcancer.org (Accessed July 14, 2020).

Zhang, M.Q., Wan, Y., Jin, Y., Xin, J.B., Zhang, J.C., Xiong, X.Z., Chen, L., Chen, G., 2014. Cigarette smoking promotes inflammation in patients with copd by affecting the polarization and survival of Th/Tregs through up-regulation of muscarinic receptor. PLoS One 9 e112350–e112350, Available at: www.plosone.org (Accessed July 17, 2020).

Zhou, L., Lopes, J.E., Chong, M.M.W., Ivanov, I.I., Min, R., Victora, G.D., Shen, Y., Du, J., Rubtsov, Y.P., Rudensky, A.Y., Ziegler, S.F., Littman, D.R., 2008. TGF-B-induced Foxp3 inhibits TH17 cell differentiation by antagonizing RORγt function. Nature 453, 236–240. Available at: /pmc/articles/PMC2597437/?report=abstract (Accessed September 28, 2020).

Zhu, J., Yamane, H., Paul, W.E., 2010. Differentiation of effector CD4 t cell populations. Annu. Rev. Immunol. 28, 445–489. Available at: /pmc/articles/PMC3502616/?report=abstract (Accessed July 16, 2020).